Romanian Reports in Physics, Vol. 64, No. 1, P. 143–154, 2012

LEARNING BY SCIENTIFIC AND EXPERIMENTAL REASONING: PRACTICAL PROMINENCE OF ERRORS AND THEIR ELIMINATION IN TOTAL INTERFERENCE CONTRAST MICROSCOPY

C. KUNCSER, A. KUNCSER, S. ANTOHE

University Bucharest, Faculty of Physics, Atomistilor Street 405, P.O. Box MG-11, Măgurele-Ilfov, 077125, Romania, E-mail: ckuncser@yahoo.com, akuncser@yahoo.com, santohe@solid.fizica.unibuc.ro

Received January 24, 2011

Abstract. An approach for teaching and learning by scientific and experimental reasoning is provided. The exemplification is given on a new version of interferometry technique, of large technological impact. The chosen example has a triple aim: (i) to familiarize the students with recent technological achievements involving the applications and the characterization of thin films and multilayers, (ii) to though and realize guided experiments rising questions about the limits of usual results derived by simple interferometry concepts and (iii) to provide the scientific reasoning and the mathematical line guides for improving the results. The described experiments solve, on a hand, real scientific issues and on the other hand, are thought as an instructional support aimed to contribute to the enhancement of the argument skills, reasoning and creativity of the students.

Key words: physics education, interferometry, TIC microscopy.

1. INTRODUCTION

Many technological achievements have been possible in our days by the sharp development of complex technologies involving thin films and multilayers [1–3]. Certainly, the multiple properties and effects appearing in such low dimensional systems are strongly dependent on structural and morphological aspects, which in turn are very sensitive to the geometrical characteristics, including also the thickness of the different components of the systems. Therefore, a comprehensive characterization of a system with respect to its macroscopic (electronic and magnetic properties) involves a complex characterization with respect to all above mentioned aspects. Standardized techniques such as X-ray diffraction (XRD) coupled with X-ray reflectometry (XRR), transmission electron microscopy (TEM), energy dispersive X-ray spectroscopy (EDX), depth profile X-ray photoemission spectroscopy (DPXPS) or Rutherford backscattering

spectroscopy (RBS) are usual techniques for analyzing the structure and stoichiometry of the layered systems together with their thickness [4]. However, such techniques are quite expensive and time-consuming. In addition, they are very precise methods suitable especially for the analysis of very low thicknesses, requiring hence, some limitations with respect to the quality of the surfaces/interfaces. For example, XRR requires strictly plane parallel layers with smooth interfaces, DPXPS the exact knowledge of the etching process parameters, RBS, the presence of a given elemental contrast, etc. A much cheaper and faster technique is the Atomic Force Microscopy (AFM) [5], but this technique has the disadvantage that involves a very sharp step of the analysed film and is too much localized with respect to the longitudinal direction along the step.

In these conditions, the microscopic interferometry could be seen as an ideal easy to operate analysis which can provide rapid information on layer morphology as well as on layer thickness, ranging from tenths of nm to a few μm. One of the newest and most performing versions of interferometry, giving information on a large range of thicknesses, is the total interference contrast microscopy. Contrary to traditional polarization interferometers working with linear polarized light, the total interference contrast (TIC) microscope works with circular polarized light [6], avoiding so the alteration of the contrast of interference pattern. The difference in the height of the specimen (*e.g.* the thickness of a thin film grown on a specific substrate) is related as usually to the difference in the optical path introduced by the reflection/transmission of the light on the step shape and can be derived by usual interferometry concepts [7]. However, additional effects could appear and influence the experimental determination and they have to be corrected, accordingly. This paper describes an experimental approach to evidence and subsequently to correct the main source of errors related to the determination of the film thickness by total contrast interferometry. At the same time, the proposed pathway, usually utilized in the scientific research, represents a good example for teaching and learning by scientific and experimental reasoning. Helping students to understand the reasoning grounding the scientific achievements and conclusions, still remains a central goal of science instruction [8]. The experiments are thought to lead to results which are in clear contradiction with the simple formula obtained by usual interferometry concepts, used in most of the text books and experimental evaluations. Reasoning and argumentation skills of the students in regard to this aspect can be investigated at this point. It is known that the argumentation is another goal of science education helping students to justify knowledge and contradiction claims [9] and therefore, the obtained experimental results can be considered as a supportive instructional context. The next step consists in the guidance of the students in solving the observed contradictions through an appropriate reasoning and an adequate mathematical approach. Finally, the conditions for solving the problem in the simplest way should be underlined. Along all the described processes, the creativity of the students should be activated.

Excepting possibilities of learning through experiment [10–12], other modern didactical methods can be complementary used in order to increase the efficiency of the educational process [13–15]. The impact of the interdisciplinarity on the Physics-Mathematics scientific education has to be also taken into account [16].

However, for the simplicity of the presentation, the paper describes unitary the proposed experiments and the progress of the scientific achievements, just as a guide for the teaching activity.

2. A BRIEF DESCRIPTION OF TIC MICROSCOPY

The principle of total interference contrast technique is based on a device induced interference pattern and the usual relationship between the differences in the height of the specimen and the corresponding optical path difference, analyzed *via* the relative displacement of the interference fringes in relation to the immediate environment.

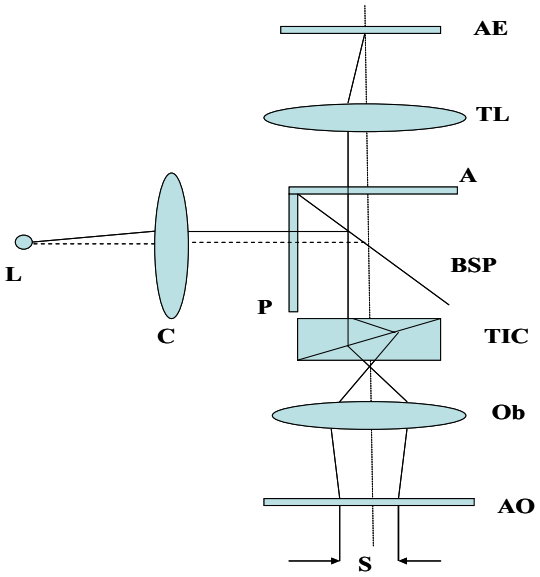

Fig. 1 – Schematic structure of a TIC mico-interferometer.

According to the scheme presented in Fig. 1, the light emitted by a source L passes through the collector C and is circularly polarized by the polarizer P. The beam splitter BSP reflects part of the polarized light through the prism TIC. This one splits the initial wave into two components propagating with just a bit deviation from a same direction. Further on, the light is focalized on the analyzed object (AO), by the object lens (Ob). After reflection on the object, the two waves

follows the reverse path, goes through the circularly analyzer A and the tube lens TL and reach the detector plane AE. The two waves, just a bit differently inclined (by the prism TIC) generates two superposed images of the object surface, which are covered by the interference fringes imposed by the optical path difference, taking increasing values from the intersection point of the two wave vectors. Maximum intensity is obtained at the intersection point where the path difference is zero, as well as at any transversal position where the path difference is an integer number of λ. The described situation is valid for any plane surface, including also a reflecting substrate. In order to obtain the thickness of the specimen, a step shape has to be introduced, *e.g.* a layer of finite lateral size has to be grown on the substrate (Fig. 2). In this situation, the observed image consists of similar interference patterns corresponding to both the surface of the reflecting substrate and the reflecting film (the inter-fringe *a* is related to the path difference, λ) which are discontinued by additional interference fringes formed just at the step region. These new fringes are shifted with respect to the previous ones belonging to the flat surfaces, by a distance *b*, due to the optical path difference, Δ, related to the film thickness, *d* (the thickness of Layer 1 in Fig. 2). Hence, the path difference, Δ, can be expressed in units of wavelengths via the general formula:

$$\Delta = \frac{b}{a}\lambda. \tag{1}$$

In order to obtain the film thickness, a relationship between Δ and *d* has to be expressed by starting from the peculiar geometrical arrangement of the experiment. According to Fig. 2, the path difference Δ, might be expressed at normal incidence (on simple geometrical grounds) as $\Delta = 2d$, and, from (1) it results straightforwardly:

$$d = \frac{\lambda}{2}\frac{b}{a}. \tag{2}$$

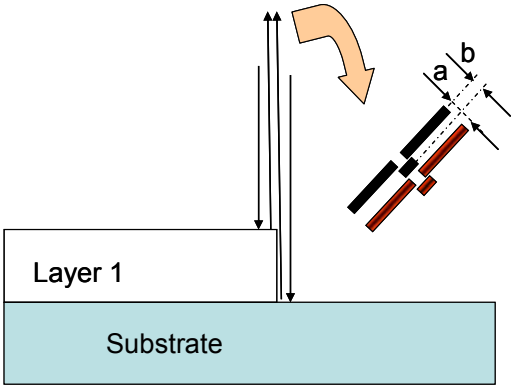

Fig. 2 – Optical path difference and interference patterns in case of normal incidence.

Equation (2) provides the film thickness when the wavelength of the radiation is known and the ratio *b/a* is obtained experimentally from the interference patterns (Fig. 2). In the following, we will exemplify by different kind of experiments that the simple equation (2) is only a first approximation and various sources of errors have to be considered. Different corrections factors and terms will be expressed after discussing and reasoning potential sources of errors. A more precise equation for the determination of the film thickness will be finally obtained.

3. EXPERIMENTAL

Two films of Cu have been grown on Si(001) substrates by rf sputtering in presence of Ar (initial vacuum of 10^{-6} mbars and rf sputtering power of 150 W). A transversal step was realized on each sample by covering a part of the Si substrate with a mask during the deposition process (Fig. 3).

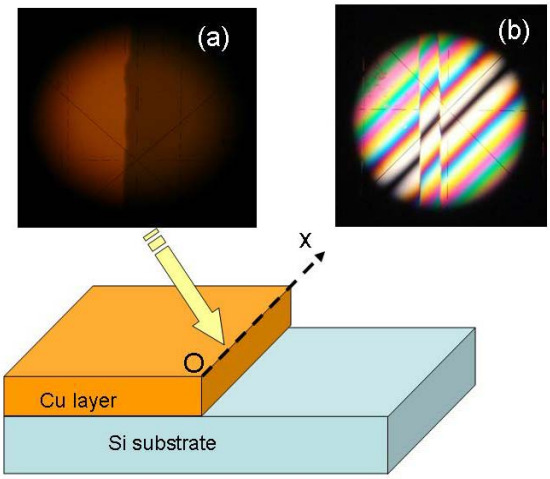

Fig. 3 – Geometry of the Test_1_Cu system and corresponding image of: a) the step; b) of the TIC interference patterns.

In the case of the first system (Test_1_Cu), the deposition time for the Cu film was 30 minutes with a discharge in an Ar pressure of $2 \cdot 10^{-2}$ mbars. In the case of the second system (Test_2_Cu), a same deposition time was used for the Cu film, but the Ar pressure was increased to $3 \cdot 10^{-2}$ mbars. The thickness of the Cu film was measured, for each sample, by an Axio Imager.D1m microscop (Karl Zeiss AG) provided with a modulator turret for total contrast interferometry. The measurements have been performed at well established coordinates along the film step (*Ox* axis in Fig. 3), defined *via* the transversal scale of the mechanical stage. A corresponding inspection of peculiar features of the step in each measuring point

was performed *via* usual reflected-light brightfield microscopy. Two sets of measurements were performed in some points, by using two different objectives, respectively, in order to observe their influence on the thickness results (the obtained values should be identical if there is no influence from the objective).

The first objective was characterized by a magnification factor of 10 and an aperture of 0.25 (code 10×/0.25) and the second by a magnification factor of 50 and an aperture of 0.80 (code 50×/0.80). The eyepiece with a magnification factor of 10 was provided with a cross like reticule connected to a digital micrometer. Typical interference patterns obtained in the TIC mode are also shown in Fig. 3. The inter-fringe and fringe-shift, a and b, respectively, are precisely measured in each point (of well defined coordinates, x_i) *via* the digital micrometer. Three sets of values were read for each position, in order to further increase the precision of the measurement (only their average values will be reported). After performing all the above mentioned measurements, an additional metallic layer (either Fe or Fe-Ni) was grown by rf sputtering on both the Cu films and the Si substrate (a representative structure is drawn in Fig. 4). On the Test_1_Cu system was grown a Fe layer, for 10 min, under the same conditions as above mentioned, resulting sample Test_1_Cu/Fe whereas on the Test_2_Cu sample was grown a Fe-Ni layer, for just 5 min, resulting sample Test_2_Cu/Fe-Ni. In principle, the difference between the top parts of the same film grown on the two sides of the step has to be identical with the thickness of the Cu layer. Hence, TIC measurements obtained on the new systems, exactly at the same coordinates along the step as in the previous determinations should provide identical thickness, unless if the type of the reflecting surface is not really significant. It is worth to mention the importance of respecting as closely as possible the coordinates of the measuring points in the two series of measurements, due to the possibility to have a not perfectly uniform step.

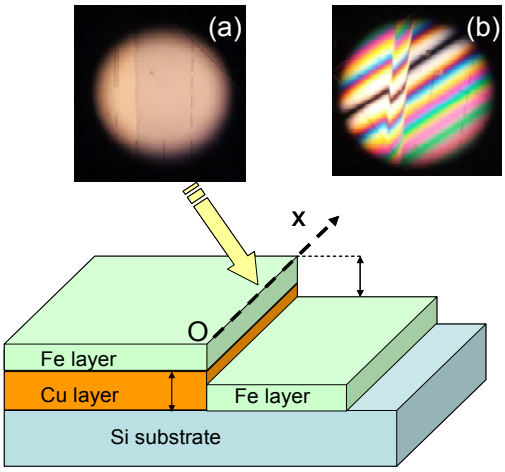

Fig. 4 – Geometry of the Test_1_Cu/Fe system and corresponding image of: a) the step; b) of the TIC interference patterns.

4. RESULTS AND DISCUSSIONS

In Figs. 5 and 6 are presented the values related to the thickness d, obtained *via* relation (2) and denoted in the following by d_0, in two different situations, respectively: (*i*) at the same coordinates of the same samples, but with two different apertures of the objective lens and (*ii*) at the same coordinates and using the same aperture of the objective lens, but before and after the deposition of the Fe or Fe-Ni layers. At only a glance of Figs. 5 and 6, it might be observed that always equation (2) leads to a lower thickness d_0, in case of a higher aperture of the objective lens, as well as in case of a same type of reflecting surface on the two sides of the step. Hence, the simple equation (2) providing the film thickness when the wavelength of the radiation is known and the ratio *b/a* is obtained experimentally from the interference patterns, is only a first approximation and additional sources of errors have to be considered. The proposed experiments prove clearly that both the aperture and the type of the reflecting surfaces on the two sides of the step have to be carefully considered and corrections of relation (2) should be provided in regard to these aspects.

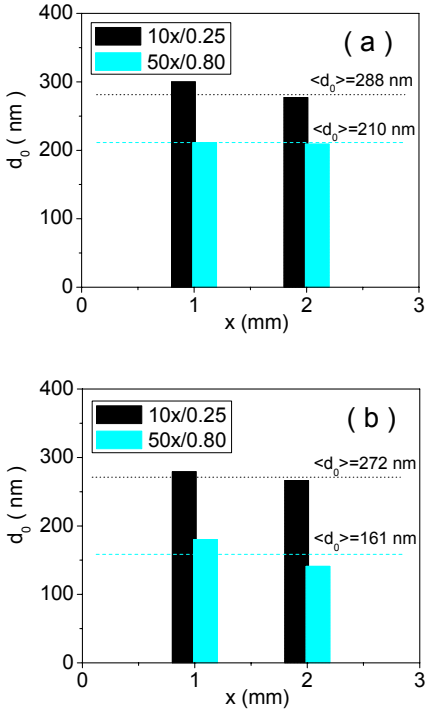

Fig. 5 – Thickness d_0 obtained on the same coordinates of sample: a) Test_1_Cu (a); b) Test_1_Cu/Fe, with two different apertures of the objective lens.

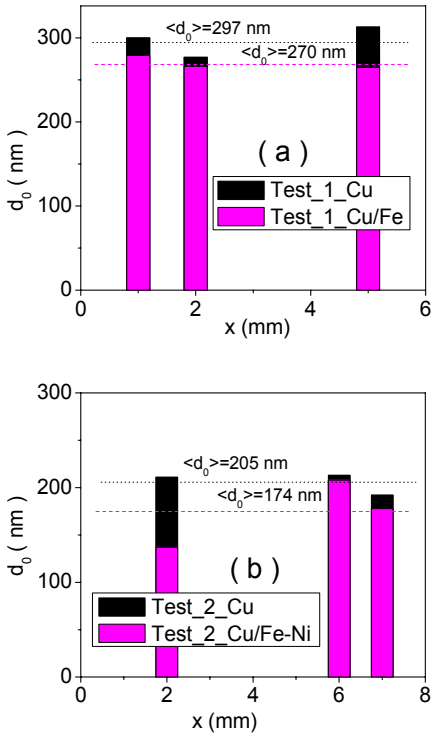

Fig. 6 – Thickness d_0 obtained with a same objective lens (10×/0.25) at the same coordinates of sample: a) Test_1; b) Test_2, before and after growing the Fe or Fe-Ni layers on the Cu layer.

Firstly, not all the radiations will present normal incidence on the stepped surface when working with finite illumination apertures and the general case of a radiation incident under an angle α should be considered. In this case, according to Fig. 7, the path difference Δ, might be expressed (on simple geometrical grounds, taking into account the thickest and the thinner paths in Fig. 7) *via* relationship:

$$\Delta = 2d / \cos\alpha - 2d \tan\alpha \sin\alpha = 2d \cos\alpha . \quad (3)$$

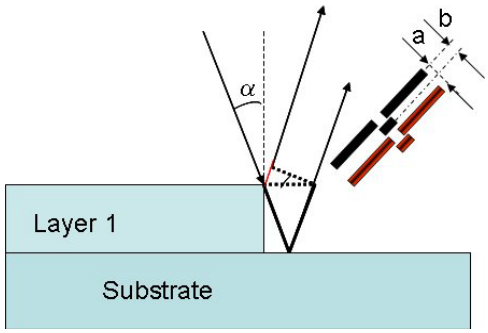

Fig. 7 – Optical path difference in case of non-perpendicular geometry, typical to finite apertures of the objective lens.

For finite apertures, angle α will take values between a minimum value of 0 and a maximum value γ, imposed by the objective aperture. In this case, relation (3) should be average over the angle α and expressed as:

$$\Delta = 2d < \cos\alpha > \quad \text{with} \quad < \cos\alpha >= \frac{\int_0^{\gamma} P(\alpha)\cos\alpha d\alpha}{\int_0^{\gamma} P(\alpha) d\alpha}. \qquad (4)$$

Hence, from relation (1), the following expression is obtained for the thickness *d*:

$$d = \frac{1}{< \cos\alpha >} \cdot \frac{\lambda}{2}\frac{b}{a} = Fd_0 \quad \text{with} \quad F = \frac{1}{< \cos\alpha >} \quad \text{and} \quad d_0 = \frac{\lambda}{2}\frac{b}{a}. \qquad (5)$$

In the above relation (5), d_0 is an equivalent thickness computed at normal incidence *via* relation (2) and *F* is an over-unity factor, as resulting from the relation $< \cos\alpha > < 1$.

The numerical estimation of $< \cos\alpha >$ and hence, of the factor *F*, becomes effective only by assuming the angular distribution $P(\alpha)$. Tacking into account that the probability to have normal incidence is decreasing for increased apertures and assuming a rotation-symmetrical illumination aperture, $P(\alpha)$ can be conveniently expressed as $P(\alpha)=\cos\alpha$ [17]. With this expression, relation (4) provides:

$$< \cos\alpha >= 2d\cos^2\frac{\gamma}{2} \quad \text{and} \quad F = \frac{1}{\cos^2\frac{\gamma}{2}} = \frac{2}{1+\cos\gamma} = \frac{2}{1+\sqrt{1-a^{*2}}}. \qquad (6)$$

In the above relation, a^* is the objective aperture, defined as $a^* = n\sin\gamma$ (n=1 for air between sample and objective) [18].

A second source of error in the expression of the path difference Δ, has to be related to the phase jump introduced by the reflection of the incident light on different types of materials. It is known that the phase jump induced by reflection is dependent on the conductive character of the reflecting surfaces [7], *e.g.* for nonconductors is about π, whereas for a conductive surface it may decreases (depending on the conductivity) with tenths of percents [17]. Having in mind Fig. 7, and relations (4) and (5), the optical path difference can be expressed as:

$$\Delta = \frac{2d}{F} + \frac{\lambda}{2\pi}(\phi_2 - \phi_1) = \frac{2d}{F} + \frac{\lambda}{2\pi}\delta\phi, \qquad (7)$$

with ϕ_2 and ϕ_1 the phase jumps on the substrate and layer 1, respectively ($\delta\phi$ is the difference of the phase jumps). Taking into account relations (1) and (7), it results:

$$d = F\frac{\lambda}{2}\frac{b}{a} - F\frac{\lambda}{2}\frac{\delta\phi}{2\pi} = F(d_0 - d_1), \tag{8}$$

with $d_0 = \frac{\lambda}{2}\frac{b}{a}$ and $d_1 = \frac{\lambda}{2}\frac{\delta\phi}{2\pi}$.

As above mentioned, d_0 is an equivalent thickness computed at normal incidence whereas d_1 is an equivalent thickness related to the phase jump. In the general expression (8) for the estimation of the step thickness d, both the aperture related correction, as well as the correction related to difference in the phase jumps are included.

Let's discuss our experimental results in the frame of relation (8) with an estimation of the factor F *via* relation (6). To the first objective lens with a^*=0.25, corresponds F = 1.018 whereas for the objective with a^* = 0.8 a factor F = 1.25 is obtained. Certainly, the correction factor F in case of working with the 10×/0.25 objective is negligible regardless the suitable form of the distribution $P(\alpha)$, leading to right estimations of the film thickness, directly *via* the equivalent thickness at normal incidence. At variance, the right thickness of the film can be computed in case of working with the 50×/0.80 objective, only by multiplying the corresponding equivalent thickness at normal incidence, d_0, by a factor F which is 1.25, for the above assumed distribution $P(\alpha)$. Hence, an equivalent thickness at normal incidence, d_0 , lower than in the case of using the 10×/0.25 objective corresponds to a same real thickness, as confirmed also by the results presented in Fig. 5.

On the other side, the equivalent thickness at normal incidence obtained with the 10×/0.25 objective on samples with the same metal on the both sides of the step (*e.g.* sample Test_1_Cu/Fe and Test_2_Cu/Fe-Ni) is a very good approximation of the real thickness, while factor F is almost 1 and d_1 is almost 0. At variance, the equivalent thickness at normal incidence, obtained by working with the same objective (F almost 1) on samples with different types of surfaces on both sides of the step (*e.g.* sample Test_1_Cu and Test_2_Cu), has to be larger (by about d_1) with respect to the equivalent thickness corresponding to the previous situation, which is confirmed by the results shown in Fig. 6.

It is worth mentioning that due to this qualitative experimental confirmation of the theoretical estimation given by relation (8), the experimental results presented in Figs. 5 and 6 could be further considered for a quantitative estimation of the factor F and the phase jump, $\delta\phi$. In this regard, firstly average values for the equivalent thickness will be considered, for an improved statistics (see the mentioned values in the figures). Secondly, the film thickness is directly estimated by the equivalent thickness at normal incidence in case of working with the 10×/0.25 objective on samples with the same metal on the both sides of the step. It results directly for the Cu film a thickness, d, of 270 nm in sample Test_1 and 174 nm in sample Test_2 (see average values of Test_1_Cu/Fe and Test_2_Cu/Fe-Ni in Fig. 6). According to relation (8) with $F = 1$ and the average values for the

equivalent thickness at normal incidence given in Fig. 6 for Test_1_Cu and Test_2_Cu, respectively, it results $d_1 = 27$ nm for the first sample and $d_1 = 31$ nm for the second one. Hence, a phase jump of 35 deg (40 deg) is directly estimated at the Cu/Si step in the Test_1(Test_2) sample, in agreement with previously reported values [17]. In a similar manner, average values reported in Fig. 5 might be considered for the estimation of the factor F associated to working objective lens of enhanced aperture. The most appropriate estimation of the Cu film thickness is $d = 270$ nm, as corresponding to the measurement with the 10×/0.25 objective on the Test_1_Cu/Fe sample. According to relation (8), it results directly a correction factor $F = 1.69$ requested by the 50×/0.80 objective. This experimental value is clearly much enhanced with respect to the theoretical estimation ($F = 1.25$) involving the angular distribution probability $P(\alpha)=\cos \alpha$.

Other types of angular distribution probabilities respecting the condition for decreased probabilities at larger angles α, might be considered for improving the agreement with the experimental results.

5. CONCLUSIONS

A complex experiment is thought and realized with both scientific and education aims. The scientific issue concerns in the prominence of errors and their elimination in total interference contrast microscopy, whereas the educational aim concerns in designing of a supportive instructional context for exercising reasoning, argumentation and creative skills of students during learning activity in laboratory. The related tasks of the experiments are: (*i*) measuring a same thickness by objectives of different apertures and by exposing different types of film surfaces, (*ii*) proving different results obtained along these cases and hence, the influence of the objective aperture and of the reflecting surface on the thickness measurements and (*iii*) finding the physical reasoning and mathematical corrections which take into account the influence of the two factors on the measured film thickness. In regard to the educational purpose, it is proposed that such instructional context following closely a real research pathway with a top technological impact, may offer very attractive and interactive laboratory courses in universities and high school excellence optional programs.

Acknowledgements. The financial support through the doctoral fellowship by the Project POSDRU 88/I.5/5/56668 is highly acknowledged.

REFERENCES

1. M. Johnson, *Magnetoelectronics* (Chs. 2 and 3), Elsevier, Amsterdam, 2004.
2. A. Fert, Jean-Marie George, H. Jaffrics, R. Mattana and P. Senor, Euro. Phys. News, **34**, *6*, 10 (2003).
3. J. F. Bobo, L. Gabillet and M.Bibes J.Phys.C: Condens.Matter, **16**, S471-96 (2004).

4. R.C. Brundle, C.A. Evans Jr., S. Wilson (ed.), *Encyclopedia of Materials Characterization – Surfaces, Interfaces, Thin Films*, Butterwarth-Heinemann, 1992.
5. C.R. Blanchard, *Atomic force microscopy – The chemical educator,* Springer-Verlang, New York Inc., 1996.
6. D. Apostol, V. Damian, P. Logofatu, Romanian Reports in Physics, **60**, *3*, 815–828 (2008).
7. F.S. Crawford Jr., *Waves; Barkeley Physics Course*, Volume 3, 1968.
8. A.E. Lawson, Sci.Ed., **94**, *2*, 336–364 (2010).
9. L.K. Berland and K. Mc Neill, Sci.Ed., **94**, *5*, 765–793 (2010).
10. M. Niculae, C.M. Niculae, E. Barna, Romanian Reports in Physics, **63**, *3*, 890–897 (2011).
11. C.G. Bostan, N. Dina, M.Bulgariu, S. Craciun, M. Dafinei, C. Chitu, I. Staicu, S. Antohe, Romanian Reports in Physics, **63**, *2*, 543–556 (2011).
12. M. Garabet, I. Neacsu, F.F. Popescu, Rom. Rep. in Physics, **62**, *4*, 918–930 (2010).
13. S. Moraru, I. Stoica, F.F. Popescu, Rom. Rep. in Physics, **63**, *2*, 577–586 (2911).
14. I. Stoica, S. Moraru, C. Miron, Rom. Rep. in Physics, **63**, *2*, 567–576 (2011).
15. L. Dinescu, C. Miron, E. Barna, Rom. Rep. in Physics, **63**, *2*, 557–566 (2011).
16. C. Miron, I. Staicu, Rom. Rep. in Physics, **62**, *4*, 906–917 (2010).
17. B.Schey, R. Danz, P. Gretscher, Photonik, **35**, *4*, (2003).
18. S.B. Ippolito, B.B. Goldberg and M.S. Ünlü, J.Appl.Phys., **97**, 0531052 (2005).